Hindawi
Adsorption Science & Technology
Volume 2023, Article ID 9398167, 13 pages
https://doi.org/10.1155/2023/9398167

Research Article

Adsorption Study and Removal of Basic Fuchsin Dye from Medical Laboratory Wastewater Using Local Natural Clay

Fuad Hama Sharif Radha,[1] Dler M. S. Shwan,[1] and Stephan Kaufhold[2]

[1]*Department of Chemistry, College of Science, University of Sulaimani, Sulaymaniyah 46001, Iraq*
[2]*Federal Institute for Geosciences and Natural Resources (BGR), Stilleweg 2, 30655 Hannover, Germany*

Correspondence should be addressed to Dler M. S. Shwan; dler.salh@univsul.edu.iq

Received 19 October 2022; Revised 12 December 2022; Accepted 4 January 2023; Published 31 March 2023

Academic Editor: Juan A. Cecilia

Local natural clay from Sulaimani zone-Takiya (TKC), Kurdistan Region of Iraq, was characterized and used for the removal of basic fuchsin (BF) dye from laboratory bacterial wastewater. The characterization of the adsorbent was carried out with XRD, XRF, and FT-IR. The clay sample was dominated by vermiculite. Adsorption tests under different conditions of contact time, pH of the solution, temperature, initial dye concentration, and adsorbent amount were performed to analyze the effect of various experimental parameters. Equilibrium time was reached within 180 minutes, and maximum BF adsorption was achieved at pH 6.8 at a temperature ranging from 20 to 50°C. The experimental data fitted the pseudo-second-order kinetic model, with the activation energy of 22.68 kJ·mol^{-1}. Adsorption isotherms could be well-fitted by the Langmuir isotherm model. The thermodynamic parameters such as ΔG°, ΔH°, and ΔS° were determined, and the negative values of ΔG° indicated that adsorption was spontaneous at all temperatures. Furthermore, the values of ΔH° indicated an endothermic reaction. Wastewater contaminated by BF dye from the bacterial laboratory was collected (BF concentration: 160 mg·L^{-1}) and treated by TKC. The resulting concentration of BF after adsorption was 4.76 mg·L^{-1}. The maximum amount of dye adsorbed is about 149.2 mg/g or 0.44 mmol/g, which is close to the range of the cation exchange capacity (CEC) value of the vermiculite which indicated that cation exchange was the dominant adsorption mechanism.

1. Introduction

Basic fuchsin (BF) is a fluorescent dye-containing mixture of rosaniline, pararosaniline, new fuchsine, and magenta II. The molecular formula is $C_{19}H_{17}N_3 \bullet HCl$, and the maximum absorption wavelength is λ-max. UV-spectrophotometry is at 546 nm. BF is used for the detection of acid-fast bacilli and is commonly used in gram staining and a mixture with phenol for acid-fast staining of mycobacterium (tuberculosis and leprosy) in the procedure described by Ziehl-Neelsen [1]. Also, BF is used as a coloring agent in the industry for textile and leather materials [2].

Wastewater contaminated by BF could be released into the environment from the sewage of the medical laboratories or the textile and leather industry. Because of their low biodegradability, some of these dyes have been reported to accumulate in surface water and sediments which may be environmentally hazardous [3]. Repeated exposure to this dye may cause toxicity and carcinogenic and mutagenic effects. In addition, its effect on the nervous system like headache, dizziness, muscle contraction, and ingestion system may cause gastrointestinal irritation with nausea and vomiting [4].

Various biological, chemical, and physical methods such as biodegradation, Fenton-biological treatment scheme, chemical oxidation, ozonolysis, filtration, ionic exchange, photodegradation, membrane technologies, coagulation/flocculation, and adsorption were tested for removing wastewater dye [5]. Although these are very efficient techniques, most of them present several drawbacks like high cost, incomplete elimination of the contaminants, and generation of sludge or by-products. Biodegradation is a low-cost method, but the bacterial strain was usually feasible for special dyes only and toxicity also posed problems for bacteria.

Also, a few biosorbents have been employed recently for the removal of BF in aqueous solutions [4, 6].

There is not much research involving the use of clay minerals for the adsorption and removal of BF from wastewater. However, related materials were tested such as modified red mud [7], natural clinoptilolite modified with apolaccase [8], and alkali-activated diatomite [9]. For these materials, the maximum adsorption capacity was 333 mg·g^{-1} (pH = 5), 2 mg·g^{-1} (pH = 6), and 10 mg·g^{-1} (pH = 6), respectively.

Among adsorbents such as fly ash [10], silica gel [11], wood [12], biogas slurry [13], activated carbon, and clay materials, clay-based materials can be considered as the most abundant and cheap raw materials which showed high adsorption capacity for colored compounds in wastewater [14, 15].

Vermiculite clay minerals are naturally occurring trioctahedral 2 : 1 phyllosilicate. They possess permanent negative charges and only partly exchangeable and hydrated interlayer ions like Ca^{2+}, Mg^{2+}, and Na^{+}. Vermiculite is a natural and modified material that was used for the adsorption and removal of many types of textile dyes from wastewater [16]. Vermiculite adsorbed 107 mg·g^{-1} of basic blue [17] and 2.2 mg·g^{-1} of pyronine Y [18]. Also, methylene blue and crystal violet onto natural vermiculite were investigated. Maximum dye loading was 0.083 and 0.103 mmol·L^{-1}, respectively [19]. Vermiculite was also used as a composite (AgI-Bi_2MoO_6/vermiculite) for the adsorptive and photocatalytic degradation of dyes [20]. In the present work, it was tried to test the adsorption and removal of BF from wastewater using locally available vermiculite. The reason for using vermiculite and not smectite is that it has a larger (negative) charge (>0.6 per formula unit), arising mostly from the substitution of Al^{3+} for Si^{4+} in tetrahedral sites [21, 22].

The hydrophobic character is a feature of BF molecules when occurs at a higher pH value, but at low pH values, its hydrophilicity and solubility are enhanced because the amino group of BF reaches the ionized state [23].

The present study is aimed at characterizing the TKC local clay and investigating the possible use of this clay as an efficient available and cheap adsorbent for wastewater treatment, due to the wide usage of BF dye and its toxicity in the wastewater.

2. Materials and Methods

2.1. Materials. Basic fuchsin (BF) is a dark green powder that will turn red in solution. Its molecular formula is $C_{19}H_{17}N_3 \bullet HCl$, and its maximum wavelength is 546 nm. Natural clay (TKC) was used in the adsorption process for the removal of basic fuchsin dye from wastewater.

2.2. Characterizations of Adsorbent. The chemical composition of the powdered TKC was determined by XRF with a PANalytical Axios spectrometer (ALMELO, Netherlands). The clay samples were prepared by mixing with a flux material (lithium metaborate Spectroflux, Flux No. 100A, Alfa Aesar) and melting into glass beads. The beads were analyzed by wavelength dispersive XRF. To determine loss on ignition (LOI), 1000 mg of sample material was heated to 1030°C for 10 min. XRD pattern was recorded using a PANalytical X'Pert PRO MPD θ-θ diffractometer (Cu-Kα radiation generated at 40 kV and 30 mA), equipped with a variable divergence slit (20 mm irradiated length), primary and secondary soller, Scientific X'Celerator detector (active length 0.59°), and a sample changer (sample diameter 28 mm). The samples were investigated from 2° to 85° 2θ with a step size of 0.0167° 2θ and a measuring time of 10 s per step. For specimen preparation, the top-loading technique was used. For the detailed clay mineralogical investigation, a texture slide of the <2 μm fraction was prepared. 15 mg per cm^2 clay was used to record an XRD scan. An aliquot of 1.5 mL of suspension was deposited on the circular (diameter = 2.4 cm) ceramic tile which was 3 mm thick. The suspension was filtered through the tile using a vacuum filter apparatus. Furthermore, the specimens were stored overnight in an ethylene glycol (EG) atmosphere at 60°C. The clay films were measured from 1° to 40° 2θ (step size 0.03° 2θ, 5 s per step) after cooling to room temperature, representing EG conditions. For measuring midinfrared spectra, the KBr pellet technique (1 mg sample/200 mg KBr) was applied. Spectra were collected on a Thermo Nicolet Nexus FTIR spectrometer (MIR beam splitter: KBr, detector DTGS TEC). The resolution was adjusted to 2 cm^{-1}. Measurements were conducted before and after drying the pellets at 150°C in a vacuum oven for 24 h. The surface emergence and microregion adsorbent before and after adsorption were measured using a scanning electron microscope (SEM, S-400 N, Hitachi).

2.3. Adsorption Studies. Adsorption experiments were carried out in batch systems to achieve the optimum operating conditions for the removal of the selected dye 0.1 g of clay mixed with 50 mL BF dye solutions of the desired concentration in 100 mL polyethylene dark bottles in a thermostatic shaker bath (GFL 1083) at the desired temperatures (20–50°C). After 5–300 min, the dispersion was centrifuged at 4000 rpm for 5 minutes to remove the clay from the solution which was spectroscopically investigated concerning its dye concentration. A Cary 60 UV-Vis spectrophotometer adjusted to 546 nm was used. The adsorption capacity (q) of the dye for each step was calculated using the following equation:

$$q = \frac{(C_o - C_e)V}{m}, \quad (1)$$

where C_o and C_e represent the initial and equilibrium concentrations (mg·L^{-1}), respectively, V is the volume of the solution (L), and m is the mass of the adsorbent (g).

The impact of the contact time was first evaluated by varying the contact time (0 to 300 min) at room temperature. The initial pH effect of the BF solution was investigated in the range from 2.0 to 11.0. Different BF concentrations (10 to 400 mg·L^{-1}) were utilized to study the impact of the initial BF concentration. The weight of the clay was varied from 0.025 to 0.25 g.

2.4. Desorption of BF from the TKC. To conduct the desorption experiments, the adsorption procedure was carried out using 0.1 g TKC with 50 mL of 150 mg·L^{-1} BF shaking for 180 minutes at 30°C. The adsorbed BF onto TKC was

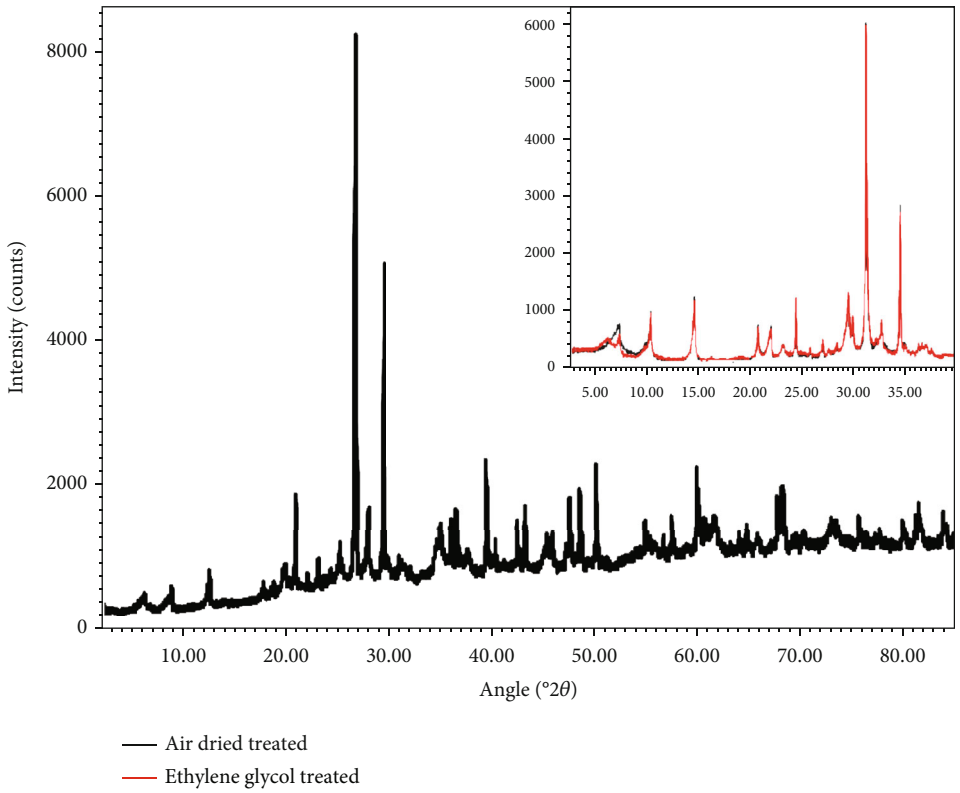

Figure 1: XRD pattern of random powder, air-dried, and EG saturated.

separated from the solutions and allowed to air-dry until it had reached a constant mass. By accounting for the dye concentrations in the solution that remained after the treatment, the amount of dye that had been absorbed was calculated. Following that, 2.00 g of dry, BF-adsorbed TKC was mixed for 1 hour with 50.0 mL of pH-adjusted water and then left to stand for 1 hour. The amount of desorption was estimated, and the concentration of BF that was leached out was calculated. For various beginning pH ranges (2-12), the desorption experiment was repeated.

3. Results and Discussion

3.1. Characterizations of Adsorbent. X-ray diffraction patterns of TKC are shown in Figure 1 for random powder, air-dried, and ethylene glycol (EG) saturated mounts. The peak observed at 14.2 Å was almost entirely shifted to 16.3 Å with EG saturated pointing towards the dominance of vermiculite [24] because smectite would shift to higher values. The powder pattern (randomly oriented mounts) proved the presence of calcite 3 Å, quartz 3.4 Å, muscovite 9 Å, and chlorite (mainly based on the (002) basal reflection at 7.1 Å and the remaining intensity at 14 Å after EG solvation).

The FTIR spectra of the TKC clay sample are dominated by a trioctahedral 2 : 1 clay mineral (vermiculite) as indicated by XRD (Figure 2). The spectra at 3622 and 3420 cm^{-1} and 3547 cm^{-1} were assigned to the OH-stretching of vermiculite and Fe-chlorite, respectively [25, 26]. OH-bending of water was determined by the bands at 1796 and 1637 cm^{-1}, while the bands at 2412, 1900, 1431, and 712 cm^{-1} were due to calcite [27]. The identification of quartz was characterized by the doublet spectra of 792 cm^{-1} and 800 cm^{-1}. The main spectral feature at about 1027 cm^{-1} was related to the Si-O stretching of all silicates present in the sample. Infrared spectroscopy confirmed the qualitative mineral composition determined by XRD. However, X-ray fluorescence (XRF) was used for determining the chemical composition of TKC, which is following XRD and IR data. The XRF values were 46.4, 0.7, 13.3, 6.4, 0.1, 4.6, 10.6, 0.7, 2.1, 14.7, and 99.8 mass% for SiO_2, TiO_2, Al_2O_3, Fe_2O_3, MnO, MgO, CaO, Na_2O, K_2O, LOI, and the sum of elements.

The morphological properties of TKC before and after BF adsorption were analyzed by using scanning electron microscopy (SEM) which is a valuable tool for precise measurement and analysis of very small features and the morphology of the sample. A flake-like TKC adsorbent particle's surface is shown in Figure 3, both before (Figure 3(a)) and after (Figure 3(b)) BF adsorption. As can be observed in Figure 3(a), TKC has a rough surface with pores that can be identified as dark spots. These pores are then filled with BF dye molecules following adsorption as shown in Figure 3(b). It was possible to see the pores becoming blocked and the material shrinking as a result of BF adsorption.

3.2. Adsorption Studies

3.2.1. Study the Effect of Contact Time. The study of the contact time effect on the adsorption of BF dye was carried out at different temperatures (Figure 4). The quick absorption of

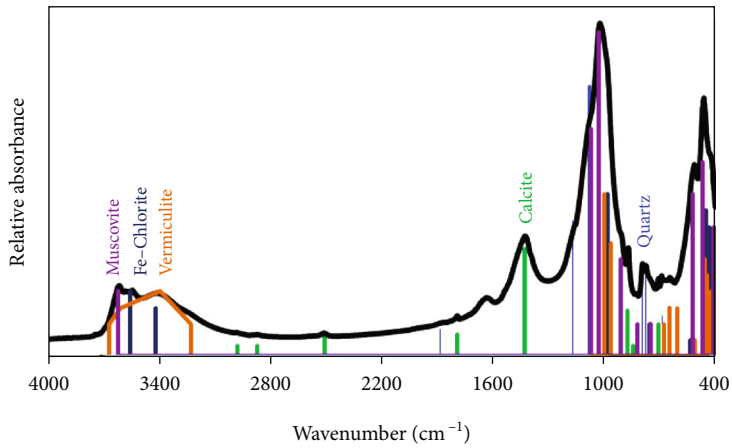

Figure 2: FTIR spectra of the TKC clay.

the dye can be noticed in the first 50th minutes of the adsorption process, which is due to the presence of a high number of empty adsorbent sites and the high affinity of solute concentration to the surface. The adsorption rate becomes slower after a period (>2 hours), and equilibrium was reached after 180 min of shaking the solution of the BF dye and TKC adsorbent at different temperatures. A 240-minute reaction time was used as a reference to ensure that equilibrium was reached and approached the constant values 72.75, 72.91, 73.5, and 73.8 mg·g^{-1} at 20, 30, 40, and 50°C. The rate of dye adsorption onto the interior sites of the adsorbent particles in batch adsorption was controlled by the adsorption of dye molecules in the bulk solution onto the interior sites of the adsorbent particles [28].

The results (Figure 4) illustrate that increasing temperature may enhance the diffusion rate of the BF molecules from the bulk solution to the adsorbent surface, which means that there is a directly proportional relationship between temperature and the adsorption capacity of BF by TKC.

3.2.2. Study the Effect of the pH of the Solution. To investigate the effect of pH on TKC adsorption capability, the study was carried out with various initial pH levels ranging from 2 to 11. The removal efficiency (percent) and adsorption capacity (mg·g^{-1}) were shown versus the various initial pH. The adsorption is found to be strongly reliant on the pH of the solution, which influences the adsorbent's surface charge, degree of ionization, and dissociation of various functional groups on the active sites [29]. The dye's highest uptake occurs at pH values greater than 4, as seen in Figure 5, which is likely due to the hydrophobic nature of BF at higher pH values.

Therefore, all the subsequent studies were performed at the normal pH of the dye which was 6.8. The clay, however, is trioctahedral, and as a result, variable charge effects are supposed to be restricted to higher pH values.

3.2.3. Point-Zero Charge (PZC) of Adsorbent. The PZC of the clay was measured using the pH drift method (Khan and Sarwar 2007). Series solutions of different pH were prepared by using HCl and NaOH; 0.1 g of the TKC was added to 50 mL of each adjusted solution in a sealed vial and equilibrated for 24 hours. The final pH was measured and plotted against the original pH; the PZC was determined as the pH at which the curve crossed the $pH_{initial} = pH_{final}$ line. This point is related to the charge on the particle's surface and is greatly influenced by the pH's effect on the charge on the TKC surface. As a result, it has an impact on a wide range of colloidal material properties, including their size and shape, stability, electrolyte interaction, suspension rheology, and ion exchange capacity.

PZC of TKC (Figure 6) also explains the reason for the high adsorption of BF around neutral pH. The TKC adsorbent surface becomes negatively charged at pH values higher than 8.2, whereas it is within the opposite state for pH < 8.2. Figure 5 shows that the adsorption of BF onto TKC is highest for PZC above 8.2, which indicates that the negative form of TKC is responsible for adsorption in this range [30].

3.2.4. Study the Effect of Adsorbent Dosage. Applying varying concentrations (0.025 to 0.25 g) of adsorbent while maintaining all other experimental conditions constant (50 mL BF dye Co = 150 mg·L^{-1}, pH = 6.8, temperature = 30°C, and 240 min equilibrium time shaking) was used to determine the adsorbent dosage influence. As shown in Figure 7, the adsorption capacity (mg·g^{-1}) and removal efficiency (percent) were plotted versus the clay weight dosage. When the overall surface area of the adsorbent (the number of adsorption sites) grows, as does the amount of the adsorbent, the percentual absorption removal of BF dye increases, until it reaches an equilibrium to approach the constant value of 74.38 mg·g^{-1} adsorption capacity, or 99.17% removal. As a result, TKC is considered a more effective adsorbent when compared to other adsorbents, such as the adsorption performance of BF on alkali-activated diatomite [9] and the use of HCl-treated malted sorghum mash [30].

3.2.5. Study the Effect of the Initial Concentration of BF Dye. The effect of the dye's initial concentration was investigated in the range of 10 to 400 mg·L^{-1}, while maintaining all other experimental conditions constant. Figure 8 shows that there is a direct proportion between the equilibrium adsorption capacity (q_e) and the initial dye concentration from 10 mg·L^{-1} to 200 mg·L^{-1}. However, the percentage removal of dye ions decreased. The higher percentual uptake at lower

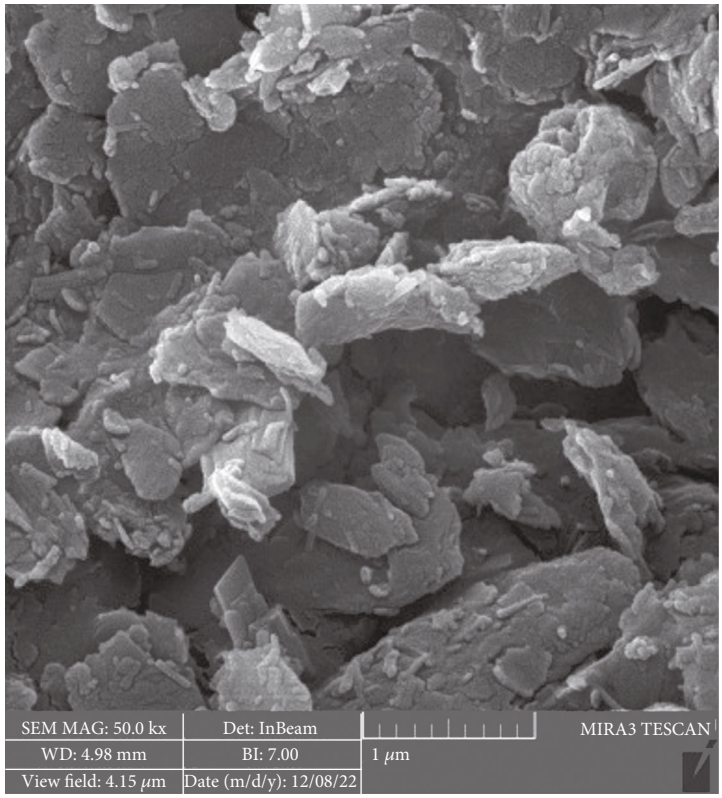

(a)

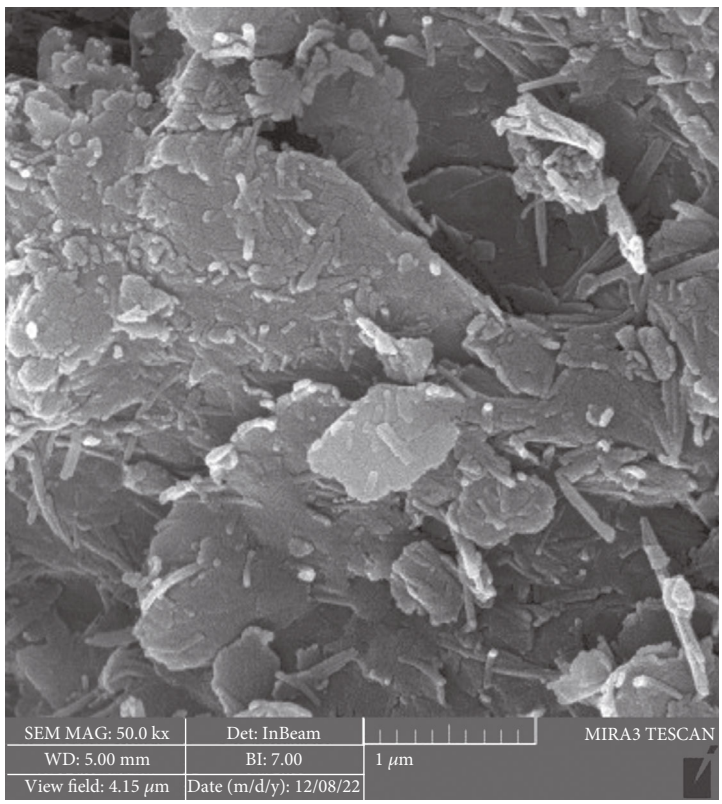

(b)

Figure 3: SEM of the TKC: (a) before BF adsorption; (b) after BF adsorption.

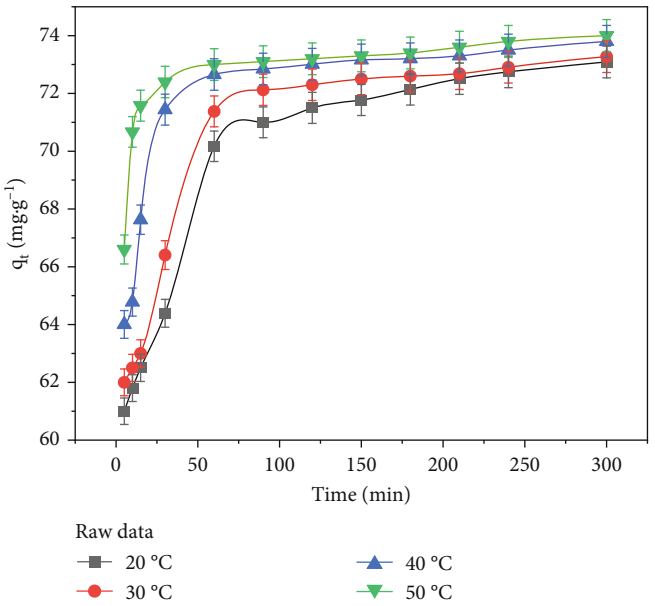

Figure 4: Effect of contact time on the adsorption of 150 mg·L^{-1} of BF dye on TKC at different temperatures.

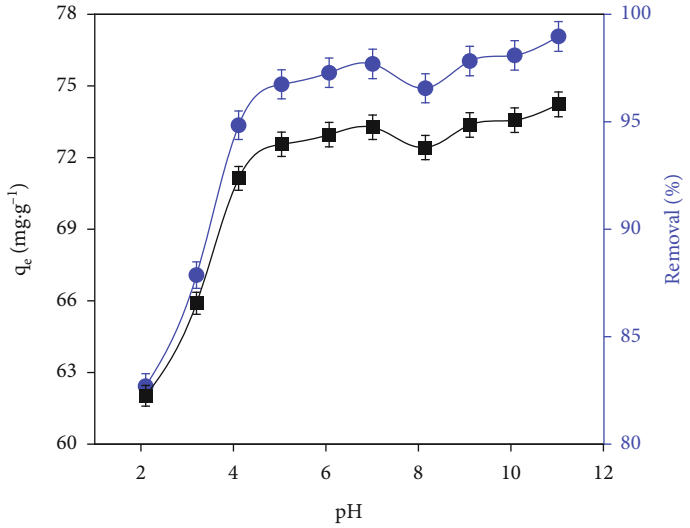

Figure 5: Effect of pH on the adsorption of 150 mg·L^{-1} of BF on TKC at 30°C.

dye concentrations was related to the available larger surface area of the adsorbent being for adsorption. While at a higher concentration of dye, the percentual uptake decreased, and this is because of the reducing number of available sites for adsorption due to saturation of adsorption sites. At a higher concentration of dye, the ratio of the initial number of moles of dye to the adsorption sites available was higher, resulting in a lower percentual removal [31].

3.2.6. Kinetic of Adsorption. The study of adsorption kinetics is significant to explore kinetic parameters (solute uptake rate determination and governs residence time or efficiency for sorption) because they can provide valuable information on the mechanism of the adsorption process. Preliminary investigations show that the adsorption kinetics at different temperatures increase with increasing contact time (Figure 9). The kinetic studies further suggest that the adsorption equilibrium was attained within about 180 min.

The two most common kinetic models, pseudo-first-order and pseudo-second-order models, were applied for adsorption kinetics.

(1) The Pseudo-First-Order Equation. Lagergren proposed this equation, which is the most common kinetics equation, and it was most significant over the initial stage of the adsorption processes [32].

The pseudo-first-order equation describes the adsorption of solid/liquid systems given as

$$q_t = q_e\left(1 - e^{-k_1 t}\right). \quad (2)$$

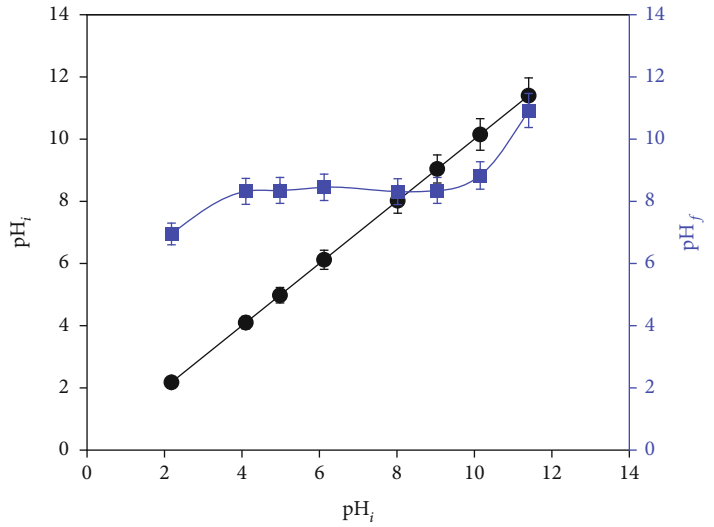

Figure 6: Determination of point of zero charges (pH_{PZC}) of the TKC by the pH drift method.

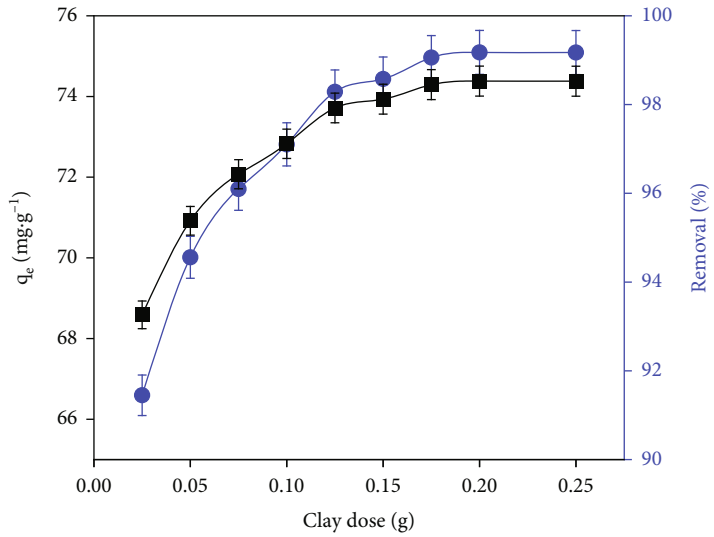

Figure 7: Effect of dosage on the adsorption of 150 mg·L^{-1} BF on TKC at 30°C.

The linearized form is

$$\log (q_e - q_t) = \log q_e - \frac{k_1}{2.303} t, \quad (3)$$

where k_1 is the pseudo-first-order rate constant (min^{-1}) of adsorption and q_e and q_t are the amounts of the BF dye (mg/g) adsorbed at equilibrium and at time t.

The Lagergren pseudo-first-order kinetic plots for the adsorption of BF dye on TKC were studied at different temperatures (Figure 9).

(2) The Pseudo-Second-Order. Both Ho and Mckay proposed this model depending on the hypothesis that the adsorption follows second-order chemisorption [33, 34].

The pseudo-second-order is assumed that the adsorption capacity is proportional to the number of binding sites occupied on the adsorbent. It is more likely to predict the behavior over the whole range of adsorption and agrees with the chemisorption mechanism being the rate-controlling step [35]. The linear form of the pseudo-second-order model is as follows:

$$\frac{t}{q_t} = \frac{1}{k_2 q_e^2} + \frac{t}{q_e}, \quad (4)$$

where q_t is the amount of adsorption at any time (mg·g^{-1}), k_2 is the rate constant of the pseudo-second-order model (g·mg^{-1}·min^{-1}), q_e is the amount of adsorption equilibrium (mg·g^{-1}), and t is the time (min).

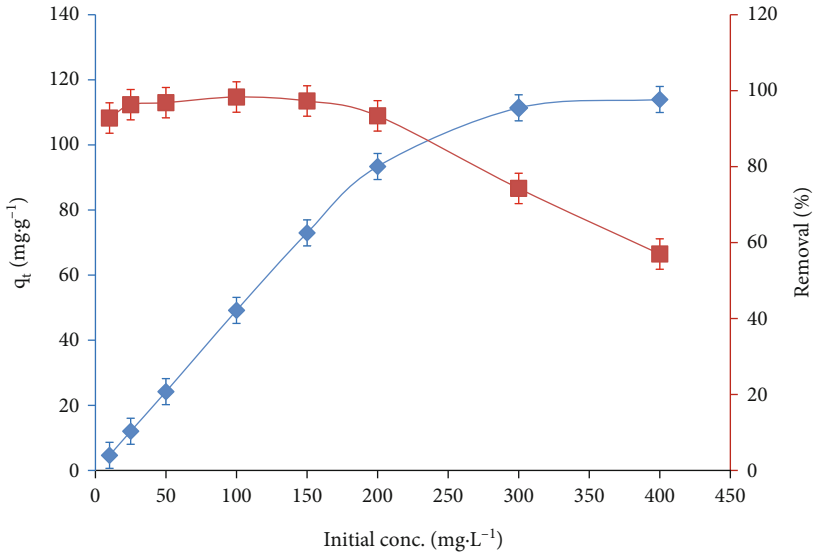

Figure 8: Effect of initial concentration on the adsorption of BF on 0.1 g of TKC at 30°C.

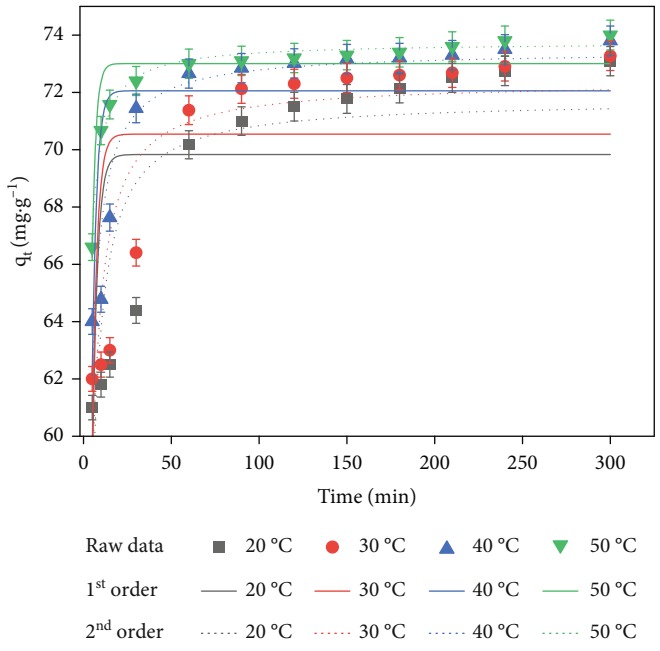

Figure 9: Nonlinear regression plots of pseudo-first-order and pseudo-second-order kinetics for the adsorption of BF dye on TKC at different temperatures.

The pseudo-first and second-order kinetic plots for the adsorption of BF dye on TKC were calculated at different temperatures as illustrated in Figure 9. Table 1 shows that the corresponding kinetic parameters were evaluated from nonlinear regression fittings, and the kinetic parameters (rate constants k_1 and k_2, correlation coefficients, and predicted ($q_{e,\,cal}$) values) are presented in Table 1.

The experimental higher value of R^2 and lower values of SSE are presented in Table 1 for the kinetic models. All of the information and the results from Figure 9 and Table 1, like the correlation coefficient values (R^2), the rate constants of the kinetic models (K_1 and K_2), and the calculated maximum adsorption capacity (q_e) from the experiment compared with that obtained from the kinetics model, show that the data were better fitted with the pseudo-second-order model as compared to the pseudo-first-order model. The result showed that the pseudo-second-order correlation coefficient values for BF adsorption onto TKC of $R^2 = 0.767$, 0.788, 0.905, and 0.983 at 293, 303, 313, and 323 K, respectively, while the pseudo-first-order correlation coefficient values of $R^2 = 0.348$, 0.356, 0.509, and 0.838 at 293, 303, 313, and 323 K, respectively. The experimental values (q_e) of BF

Table 1: Kinetic model parameters for the adsorption of BF on TKC.

Kinetic models	Kinetic parameters	Temperature (K)			
		293	303	313	323
	q_{exp} (mg·g^{-1})	149.5	167.5	177.5	186.3
Pseudo 1st order	q_{calc} (mg·g^{-1})	69.83106 ± 1.26091	70.54346 ± 1.19893	72.05584 ± 0.80815	73.00539 ± 0.26722
	k_1 (min^{-1})	0.47594 ± 0.02687	0.39655 ± 0.05393	0.37066 ± 0.07084	0.36236 ± 0.07184
	R^2	0.348	0.356	0.509	0.838
	SSE	163.3	148.1	67.9	7.6
Pseudo 2nd order	q_{calc} (mg·g^{-1})	73.75046 ± 0.10077	73.45156 ± 0.4151	72.37468 ± 0.80579	71.72428 ± 0.88367
	k_2 (g·mg^{-1}·min^{-1})	0.02653 ± 0.00122	0.01478 ± 0.00175	0.01159 ± 0.00223	0.01112 ± 0.00229
	R^2	0.767	0.788	0.905	0.983
	SSE	58.4	48.7	13.2	0.8

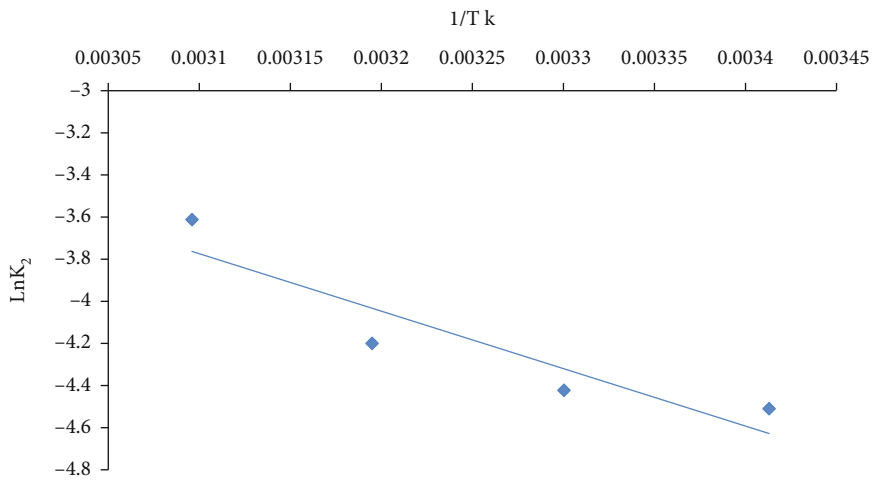

Figure 10: Plot of LnK_2 versus $1/T$ (K) for BF on KTC adsorbent.

onto TKC were 149.5, 167.5, 177.5, and 186.3 g. g^{-1} at 293, 303, 313, and 323 K, respectively, which were closer to that obtained from the pseudo-second-order kinetics model as compared to that of the pseudo-first-order. Also, the fast-kinetic adsorption of AFD in the first 30 minutes followed by gradual adsorption can be seen from the rate constant from both the pseudo-first-order and pseudo-second-order. The value of K_1 and K_2 was determined, indicating that the faster rate of adsorption is more directed towards that of the pseudo-second-order.

The study of the temperature effect on the rate at which BF is adsorbed from solution also allows for an evaluation of the activation energy (Ea) for the sorption reaction; the Ea can be calculated from the Arrhenius equation:

$$k_2 = Ae^{-E_a/\mathrm{RT}}. \quad (5)$$

The E_a value was calculated from the slope of the plot of ln k_2 vs. $1/T$ (Figure 10), according to the Arrhenius equation (Equation (6)).

$$\ln k_2 = \ln A - \frac{E_a}{\mathrm{RT}}, \quad (6)$$

where E_a (J·mol^{-1}), A (g·mol^{-1}·s^{-1}), K_2 (g·mol^{-1}·s^{-1}), R (8.314 J·K^{-1}·mol^{-1}), and $T(k)$ are the activation energy of the adsorption and the Arrhenius per-exponential factor, rate constant for pseudo-second-order, and the gas constant and temperature, respectively.

Low activation energies (<40 kJ·mol^{-1}) indicate the physical nature of the adsorption process, while the value of E_a (>80 kJ·mol^{-1}) indicates chemisorption. In the present case, E_a was found to be (22.68 kJ·mol^{-1}) which is consistent with physisorption [14].

3.2.7. Adsorption Isotherms. Investigating the mechanism of the adsorption process depends on the distribution of the adsorbate between solution and adsorbent at equilibrium conditions when the dynamic balancing between the concentrations of adsorbate in bulk solution with that of the interface is established. The data obtained from the sorption equilibrium can be used to acquire the adsorption capacity and certain constants whose values express the surface properties and affinity of a sorbent.

In the present study, Langmuir and Freundlich's isotherm parameters were used for the interpretation of the equilibrium adsorption data.

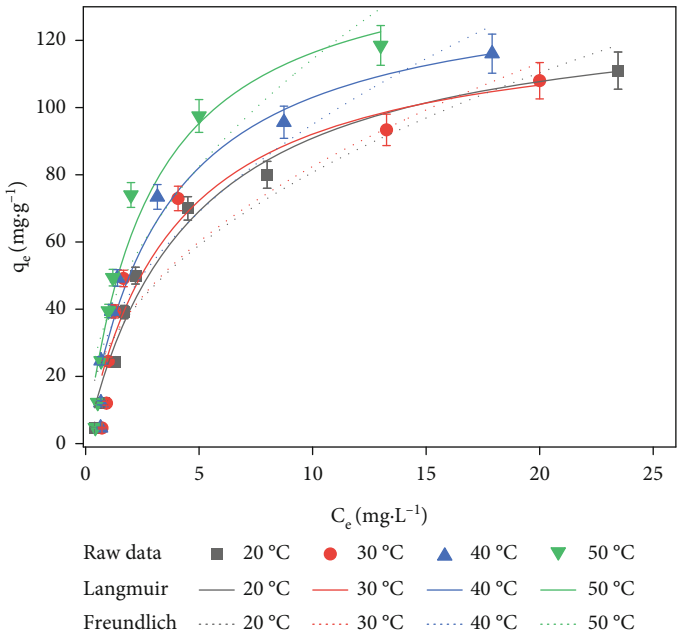

Figure 11: The Langmuir and Freundlich isotherm models for the adsorption of BF dye on TKC at different temperatures (0.1 g TC, initial pH = 6.0).

Table 2: Isotherm parameters for the adsorption of BF dye onto TKC adsorbent.

Isotherm models	Isotherm parameters	Temperature (K)			
		293	303	313	323
Langmuir	q_m (mg·g^{-1})	132.30323 ± 9.3445	126.75118 ± 13.68696	138.08058 ± 14.21631	149.16508 ± 15.80561
	K_L (L mg^{-1})	0.21934 ± 0.0377	0.26587 ± 0.07655	0.29393 ± 0.07778	0.35393 ± 0.08827
	R_L	0.029	0.024	0.022	0.018
	R^2	0.977	0.935	0.947	0.951
	SSE	213.2	653.6	593.4	572.5
Freundlich	K_F (mg·g^{-1}) (L·mg^{-1})	28.52537 ± 4.66085	28.74579 ± 5.86427	32.76571 ± 5.95929	38.49453 ± 6.56976
	n_f	2.21404 ± 0.3234	2.18457 ± 0.39493	2.16319 ± 0.36822	2.11376 ± 0.38198
	R^2	0.910	0.876	0.884	0.863
	SSE	835.6	1244.6	1297.6	1600.2

The Langmuir isotherm model assumes that monolayer adsorption of the adsorbate over specific homogenous sites on the adsorbent surface occurs due to the certain number of fixed adsorption sites with equivalent properties [36].

The Langmuir isotherm can be expressed in the following equation (Equation (7)):

$$q_e = \frac{q_m K_L C_e}{1 + K_L C_e}, \quad (7)$$

@where q_e and q_m are the amounts of the adsorbate adsorbed per unit weight of clay (mg·g^{-1}) at equilibrium and monolayer saturation, respectively, K_L is the Langmuir equilibrium constant, and C_e is the concentration of the adsorbate in solution at equilibrium (mg·L^{-1}).

The values of K_L and q_m were calculated from the nonlinear regression analysis at different temperatures (Figure 11 and Table 2). The maximum dye adsorption capacity by TKC was found to be 149.2 mg·g^{-1} or 0.44 mmol·g^{-1} at 50°C, which is close to the range of the CEC value of the vermiculite. Therefore, the main adsorption mechanism is cation exchange which is not surprising since the molecule is similar to other index cations that could be adsorbed by the clay. The values of K_L increased with increasing temperature, indicating that increasing temperature induced a higher maximum adsorption capacity.

The essential feature of the Langmuir isotherm can be expressed in terms of a dimensionless factor called separation factor also called equilibrium parameter (R_L) which is shown in the following equation [37]:

$$R_L = \frac{1}{1 + K_L C_0}, \quad (8)$$

Table 3: Thermodynamic parameters for the adsorption of BF dye onto TKC.

C_o (mg·L^{-1})	ΔH° (kJ·mol^{-1})	ΔS° (kJ·mol^{-1})	ΔG° (kJ·mol^{-1})			
			293 K	303 K	313 K	423 K
50	18.59	0.09	-7.22	-8.10	-8.98	-9.86
100	15.99	0.08	-7.62	-8.43	-9.23	-10.04

where K_L is the Langmuir constant and C_o is the initial concentration of the adsorbate. The shape of the isotherm indicates by the value of R_L to be either unfavorable ($R_L > 1$), linear ($R_L = 1$), favorable ($0 < R_L < 1$), or irreversible ($R_L = 0$).

The Freundlich equation is an empirical equation that describes multilayer adsorption of the adsorbate on a heterogeneous adsorbent surface. Equation (9) represents the linearized Freundlich isotherm [38].

$$q_e = K_f + C_e^{1/n}, \tag{9}$$

@where K_f and n are the Freundlich constants representing adsorption capacity and intensity, respectively.

The adsorption capacity K_f increased directly proportional to increasing temperature as represented in Table 2. The magnitude of n values (that gives a measure of the favorability of adsorption) between 1 and 10 ($1/n$ less than 1) represents favorable adsorption. In the present study, the value of n presented the same trend, indicating favorable adsorption [2].

Based on the high correlation coefficient R^2, it has been deduced that the Langmuir model is better fitted to the experimental data.

3.2.8. Thermodynamic Studies. The effect of temperature on the adsorption is important to estimate the thermodynamic parameters such as ΔG°, ΔH°, and ΔS°, which are useful in determining whether the adsorption reaction is endothermic or exothermic and the spontaneity of the adsorption process.

The Gibbs free energy ΔG° (kJ·mol^{-1}) of adsorption was determined from the following equation:

$$\Delta G^\circ = -\mathrm{RT}\ln Kc. \tag{10}$$

Standard entropy change ΔS° (kJ·mol^{-1}·K^{-1}) and standard enthalpy change ΔH° (kJ·mol^{-1}) of the adsorption process can be found from the van't Hoff equation as shown as follows:

$$\begin{aligned} \Delta G^\circ &= \Delta H^\circ - T\Delta S^\circ, \\ \ln Kc &= \frac{\Delta S^\circ}{R} - \frac{\Delta H^\circ}{RT}. \end{aligned} \tag{11}$$

Kc is calculated using the following equation:

$$Kc = \frac{Cs}{Ce}, \tag{12}$$

where K_c is the equilibrium constant and C_s and C_e are the equilibrium concentration (mg·L^{-1}) of the dye on the adsorbent and in the solution, respectively [39].

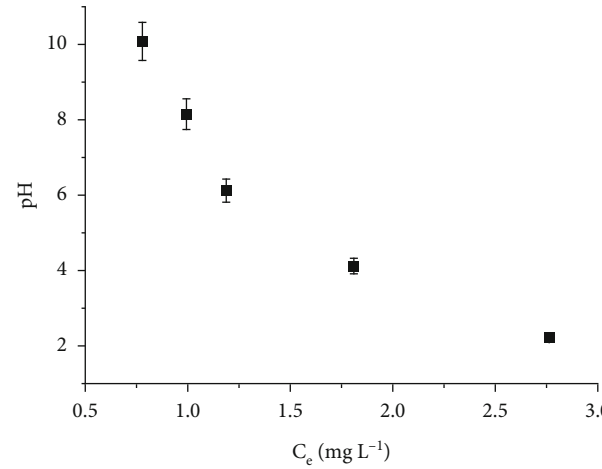

Figure 12: Concentrations obtained for desorbed BF dye at different initial solution pH values.

The values of the thermodynamic parameters are presented in Table 3. The negative value of ΔG° at all temperatures indicates the feasibility and spontaneity while the positive value of ΔH° substantiates the endothermic nature of the adsorption process. Also, if the ΔS° value is positive, the process would become more spontaneous on raising the temperature [40].

The positive value of ΔS° indicates that some structural changes may have taken place due to the affinity of interactions of dye molecules with active groups in the clay surface; therefore, the randomness at the solid/liquid interface during the adsorption is increased, despite the liberate inorganic cations from the clay causing an overall increase in entropy analogous [14, 41].

4. Desorption Study

A desorption study was conducted by altering the starting solution pH to examine the ability of adsorbed BF dye to leach into the solution under various conditions. Figure 12 displays the concentrations for samples desorbed with distilled water at various medium pH levels following preadsorption of a mixture of synthetic dye effluents with a concentration of 150 mg·L^{-1}. The results show that the desorption considerably increases at pH values below 2.5 and decreases with increasing medium pH. The reason why BF dye adsorbed on TKC is probably that BF is hydrophobic at higher pH values, as mentioned in the adsorption of dye with increasing pH of the medium, confirming the research's results. Therefore, highly acidic media are preferred for desorption. However, the reusability of the TKC is somewhat problematic, and further research is required.

More importantly, desorption experiments show that the BF dye adsorbed on the TKC adsorbent will not leach to the environment under normal conditions.

5. Applications on Real Samples

The BF-containing wastewater samples (laboratory wastewater) were taken from the Medical Laboratory Science (MLS) Department of Komar University, as a true sample for the remediation application of wastewater through the use of TKC natural clay. The real samples include detectable (BF) with a noticeable amount ($160\,mg{\cdot}L^{-1}$) of BF depending on whether the used amount of distilled water was for washing and liberating the excess of the BF that was used in excess for coloring the bacteria species. The pH of the wastewater (real) samples was measured and was found in the range of 7.2–7.7. Adsorption tests were carried out using the TKC described in the current work. The final concentration following adsorption of BF after adsorption onto TKC was $4.76\,mg{\cdot}L^{-1}$. These results showed that the adsorbent was capable to eliminate BF from wastewater (real samples) at a rate of greater than 97%.

6. Conclusion

The surface of natural local clay (TKC) is a more effective adsorbent for the removal of hydrophilic organic compounds such as basic fuchsin dye from aqueous solution; this is due to the electrically charged and hydrophilic characteristics of the surface. The parameters that affected the adsorption such as pH, contact time, temperature, adsorbent dose, and initial dye concentration were determined. The influence of the initial pH of the solution on the adsorption showed a significant effect, and the efficient pH was obtained at the normal pH of the BF dye (pH = 6.8). The maximum amount of dye adsorbed is about $149.2\,mg{\cdot}g^{-1}$ or $0.44\,mmol{\cdot}g^{-1}$, which is close to the CEC value of the vermiculite. Cation exchange, hence, is supposed to be the dominant adsorption mechanism which is also in agreement with the kinetic and thermodynamic results. The negative value of ΔG° indicated spontaneity at study temperatures, and the positive values of ΔS° show the affinity of the adsorbent to the adsorbate. The positive values of ΔH° and the adsorption of the dye are favorably influenced by the increase in temperature indicating the endothermic nature of the adsorption process. Also, the sorption kinetics followed the pseudo-second-order model. The calculated activation energy for the adsorption is $22.68\,kJ{\cdot}mol^{-1}$ indicating that the adsorption falls in the range of a physisorption process and has a low potential barrier. The results of the present investigation indicate that TKC has a suitable adsorption capacity for the removal of BF dye in wastewater. These results, therefore, are of great importance for the removal of toxic dyes from wastewater and sewage and applied to real sample wastewater.

Data Availability

The authors confirm that the data supporting the findings of this study are available within the article.

Conflicts of Interest

The authors declare that they have no conflicts of interest.

Authors' Contributions

F. Radha, D. Shwan, and S. Kaufhold were responsible for the conceptualization. D. Shwan was responsible for the methodology. D. Shwan and S. Kaufhold were responsible for the software. D. Shwan and S. Kaufhold were responsible for the validation. F. Radha and D. Shwan were responsible for the formal analysis. D. Shwan and S. Kaufhold were responsible for the investigation. F. Radha and D. Shwan were responsible for the resources. F. Radha, D. Shwan, and S. Kaufhold were responsible for the data curation. F. Radha and D. Shwan were responsible for the writing—original draft preparation. D. Shwan and S. Kaufhold were responsible for the writing—review and editing. F. Radha and D. Shwan were responsible for the visualization. D. Shwan and S. Kaufhold were responsible for the supervision. All of the authors worked on the manuscript, read the final version, and approved it.

Acknowledgments

We gratefully acknowledge the Komar University, MLS Department, for providing the real sample for the application of the present study and all who contributed to the conduction of this study especially Mr. Karokh B. Ali, Hassan H. Amin, and Dlzar D. Ghafoor.

References

[1] M. El-Azazy, A. S. El-Shafie, A. Ashraf, and A. A. Issa, "Eco-structured biosorptive removal of basic fuchsin using pistachio nutshells: a definitive screening design-based approach," *Applied Sciences*, vol. 9, no. 22, p. 4855, 2019.

[2] M. El Haddad, "Removal of basic fuchsin dye from water using mussel shell biomass waste as an adsorbent: equilibrium, kinetics, and thermodynamics," *Journal of Taibah University for Science*, vol. 10, no. 5, pp. 664–674, 2016.

[3] H. S. Rai, S. Singh, P. P. S. Cheema, T. K. Bansal, and U. C. Banerjee, "Decolorization of triphenylmethane dye-bath effluent in an integrated two- stage anaerobic reactor," *Journal of Environmental Management*, vol. 83, no. 3, pp. 290–297, 2007.

[4] V. K. Gupta, A. Mittal, V. Gajbe, and J. Mittal, "Adsorption of basic fuchsin using waste materials–bottom ash and deoiled soya –as adsorbents," *Journal of Colloid and Interface Science*, vol. 319, no. 1, pp. 30–39, 2008.

[5] E. Kalkan, H. Nadaroglu, N. Celebi, H. Celik, and E. Tasgin, "Experimental study to remediate acid fuchsin dye using laccase-modified zeolite from aqueous solutions," *Polish Journal of Environmental Studies*, vol. 24, no. 1, pp. 115–124, 2015.

[6] A. D. Sponza, N. J. Fernandez, D. Yang, K. A. Ortiz, and A. E. Navarro, "Comparative sorption of methylene blue onto hydrophobic clays," *Environments*, vol. 2, no. 4, pp. 388–398, 2015.

[7] H. Nadaroglu, E. Kalkan, and N. Celebi, "Adsorption performance of laccase modified-red mud for acid fuchsin dye removal from aqueous solutions," *Annals of Chromatography and Separation Techniques*, vol. 3, no. 1, p. 1027, 2017.

[8] H. Nadaroglu, E. Kalkan, and N. Celebi, "Removal of reactive black 5 from wastewater using natural clinoptilolite modified with apolaccase," *Clay Minerals*, vol. 50, pp. 65–76, 2015.

[9] Y. Zhao, J. Geng, J. Cai, Y. F. Cai, and C. Y. Cao, "Adsorption performance of basic fuchsin on alkali-activated diatomite," *Adsorption Science & Technology*, vol. 38, no. 5-6, pp. 151–167, 2020.

[10] G. S. Gupta, G. Prasad, K. K. Panday, and V. N. Singh, "Removal of chrome dye from aqueous solutions by fly ash," *Water, Air, and Soil Pollution*, vol. 37, pp. 13–24, 1988.

[11] M. N. Ahmed and R. N. Ram, "Removal of basic dye from waste-water using silica as adsorbent," *Environmental Pollution*, vol. 77, no. 1, pp. 79–86, 1992.

[12] Y. S. Ho and G. McKay, "Kinetic models for the sorption of dye from aqueous solution by wood," *Process Safety and Environmental Protection*, vol. 76, no. 2, pp. 183–191, 1998.

[13] R. T. Yamuna and C. Namasivayam, "Color removal from aqueous solution by biogas residual slurry," *Toxicological and Environmental Chemistry*, vol. 38, no. 3–4, pp. 131–143, 1993.

[14] C. A. P. Almeida, N. A. Debacher, A. J. Downs, L. Cottet, and C. A. D. Mello, "Removal of methylene blue from colored effluents by adsorption on montmorillonite clay," *Journal of Colloid and Interface Science*, vol. 332, no. 1, pp. 46–53, 2009.

[15] Z. Bouberka, A. Khenifi, N. Benderdouche, and Z. Derriche, "Removal of supranol yellow 4GL by adsorption onto Cr-intercalated montmorillonite," *Journal of Hazardous Materials*, vol. 133, no. 1–3, pp. 154–161, 2006.

[16] D. M. Salh, B. K. Aziz, and S. Kaufhold, "High adsorption efficiency of Topkhana natural clay for methylene blue from medical laboratory wastewater: a Linear and Nonlinear Regression," *Silicon*, vol. 12, no. 1, pp. 87–99, 2020.

[17] Y. S. Choi and J. H. Cho, "Color removal from dye wastewater using vermiculite," *Environmental Technology*, vol. 17, no. 11, pp. 1169–1180, 1996.

[18] M. Toprak, A. Salci, and A. R. Demirkiran, "Comparison of adsorption performances of vermiculite and clinoptilolite for the removal of pyronine Y dyestuff," *Reaction Kinetics, Mechanisms and Catalysis*, vol. 111, no. 2, pp. 791–804, 2014.

[19] X. Yu, C. Wei, and H. Wu, "Effect of molecular structure on the adsorption behavior of cationic dyes onto natural vermiculite," *Separation and Purification Technology*, vol. 156, pp. 489–495, 2015.

[20] F. Papers, "Efficient adsorption and photocatalytic degradation of dyes by AgI-Bi_2MoO_6/Vermiculite composite under visible Light," *ChemistrySelect*, vol. 4, no. 41, pp. 12022–12031, 2019.

[21] M. F. Brigatti, E. Galán, and B. K. G. Theng, "Structure and mineralogy of clay minerals," *Developments in Clay Science*, vol. 5, 2013.

[22] W. Bleam, "Clay Mineralogy and Chemistry," *Soil and Environmental Chemistry*, vol. 2, pp. 87–146, 2017.

[23] R. Lan, J. Li, and B. Chen, "Ultrasonic degradation of fuchsin basic in aqueous solution: effects of operating parameters and additives," *International Journal of Photoenergy*, vol. 2013, Article ID 893131, 7 pages, 2013.

[24] R. Cruz, "Chemical and structural evolution of 'metamorphic vermiculite' in metaclastic rocks of the Betic Cordillera, Málaga, Spain: a synthesis," *The Canadian Mineralogist*, vol. 44, no. 1, pp. 249–265, 2006.

[25] M. Arab, D. Bougeard, and K. S. Smirnov, "Experimental and computer simulation study of the vibrational spectra of vermiculite," *Physical Chemistry Chemical Physics*, vol. 4, no. 10, pp. 1957–1963, 2002.

[26] S. Hillier and B. Velde, "Chlorite interstratified with a 7 Å mineral: an example from offshore Norway and possible implications for the interpretation of the composition of diagenetic chlorites," *Clay Minerals*, vol. 27, no. 4, pp. 475–486, 1992.

[27] F. A. Andersen, L. Brecevic, G. Beuter et al., "Infrared spectra of amorphous and crystalline calcium carbonate," *Acta Chemica Scandinavica*, vol. 45, pp. 1018–1024, 1991.

[28] S. Banerjee and M. C. Chattopadhyaya, "Adsorption characteristics for the removal of a toxic dye, tartrazine from aqueous solutions by a low cost agricultural by-product," *Arabian Journal of Chemistry*, vol. 10, pp. S1629–S1638, 2017.

[29] M. Wawrzkiewicz and Z. Hubicki, "Removal of tartrazine from aqueous solutions by strongly basic polystyrene anion exchange resins," *Journal of Hazardous Materials*, vol. 164, no. 2-3, pp. 502–509, 2009.

[30] E. O. Oyelude, F. Frimpong, and D. Dawson, "Studies on the removal of basic fuchsin dye from aqueous solution by HCl treated malted sorghum mash," *Journal of Materials and Environmental Science*, vol. 6, no. 4, pp. 1126–1136, 2015.

[31] P. Taylor, D. Prabu, R. Parthiban, P. S. Kumar, N. Kumari, and P. Saikia, "Desalination and water treatment adsorption of copper ions onto nano-scale zero-valent iron impregnated cashew nut shell," *Desalination and Water Treatment*, vol. 57, no. 14, pp. 37–41, 2016.

[32] P. K. Baskaran, B. R. Venkatraman, and S. Arivoli, "Kinetics of adsorption of ferrous ion onto acid activated carbon from Zea mays dust," *E-Journal of Chemistry*, vol. 8, no. 1, pp. 185–195, 2011.

[33] Y. S. Ho, "Citation review of Lagergren kinetic rate equation on adsorption reactions," *Scientometrics*, vol. 59, no. 1, pp. 171–177, 2004.

[34] Y. S. Ho and G. Mckay, "Pseudo-second order model for sorption processes," *Process Biochemistry*, vol. 34, no. 5, pp. 451–465, 1999.

[35] M. S. Chiou and H. Y. Li, "Adsorption behavior of reactive dye in aqueous solution on chemical cross- linked chitosan beads," *Chemosphere*, vol. 50, no. 8, pp. 1095–1105, 2003.

[36] M. H. Armbruster and J. B. Austin, "The adsorption of gases on plane surfaces of mica," *Journal of the American Chemical Society*, vol. 60, no. 2, pp. 467–475, 1938.

[37] S. N. Hurairah, N. M. Lajis, and A. A. Halim, "Methylene blue removal from aqueous solution by adsorption on Archidendron jiringa seed shells," *Journal of Geoscience and Environment Protection*, vol. 8, no. 2, pp. 128–143, 2020.

[38] J. Appel, "Freundlich's adsorption isotherm," *Surface Science*, vol. 39, no. 1, pp. 237–244, 1973.

[39] A. K. Meena, K. Kadirvelu, G. K. Mishraa, C. Rajagopal, and P. N. Nagar, "Adsorption of Pb(II) and Cd(II) metal ions from aqueous solutions by mustard husk," *Journal of Hazardous Materials*, vol. 150, no. 3, pp. 619–625, 2008.

[40] L. Cottet, C. A. P. Almeida, N. Naidek, M. F. Viante, M. C. Lopes, and N. A. Debacher, "Adsorption characteristics of montmorillonite clay modified with iron oxide with respect to methylene blue in aqueous media," *Applied Clay Science*, vol. 95, pp. 25–31, 2014.

[41] S. Hong, C. Wen, J. He, F. Gan, and Y. S. Ho, "Adsorption thermodynamics of methylene blue onto bentonite," *Journal of Hazardous Materials*, vol. 167, no. 1–3, pp. 630–633, 2009.